BIOCHEMISTRY
including biophysical chemistry & molecular biology
Article

Biochemistry **2010,** *49,* 5035–5041 5035
DOI: 10.1021/bi100610e

Identification of a Hypothetical Protein from *Podospora anserina* as a Nitroalkane Oxidase[†,‡]

José R. Tormos,[§] Alexander B. Taylor,[§] S. Colette Daubner,[∥] P. John Hart,[§,⊥] and Paul F. Fitzpatrick*[,§,#]

[§]*Department of Biochemistry, University of Texas Health Science Center, San Antonio, Texas 78229,* [∥]*Department of Biology, St. Mary's University, San Antonio, Texas 78228,* [⊥]*Department of Veterans Affairs, Audie Murphy Division, Geriatric Research, Education, and Clinical Center, South Texas Veterans Health Care System, San Antonio, Texas 78229, and* [#]*Department of Chemistry, University of Texas, San Antonio, San Antonio, Texas 78249*

Received April 21, 2010; Revised Manuscript Received May 17, 2010

ABSTRACT: The flavoprotein nitroalkane oxidase (NAO) from *Fusarium oxysporum* catalyzes the oxidation of primary and secondary nitroalkanes to their respective aldehydes and ketones. Structurally, the enzyme is a member of the acyl-CoA dehydrogenase superfamily. To date no enzymes other than that from *F. oxysporum* have been annotated as NAOs. To identify additional potential NAOs, the available database was searched for enzymes in which the active site residues Asp402, Arg409, and Ser276 were conserved. Of the several fungal enzymes identified in this fashion, PODANSg2158 from *Podospora anserina* was selected for expression and characterization. The recombinant enzyme is a flavoprotein with activity on nitroalkanes comparable to the *F. oxysporum* NAO, although the substrate specificity is somewhat different. Asp399, Arg406, and Ser273 in PODANSg2158 correspond to the active site triad in *F. oxysporum* NAO. The k_{cat}/K_M−pH profile with nitroethane shows a pK_a of 5.9 that is assigned to Asp399 as the active site base. Mutation of Asp399 to asparagine decreases the k_{cat}/K_M value for nitroethane over 2 orders of magnitude. The R406K and S373A mutations decrease this kinetic parameter by 64- and 3-fold, respectively. The structure of PODANSg2158 has been determined at a resolution of 2.0 Å, confirming its identification as an NAO.

The flavoenzyme nitroalkane oxidase (NAO)[1] from the soil fungus *Fusarium oxysporum* catalyzes the oxidation of nitroalkanes to the corresponding aldehydes or ketones with the release of nitrite and the consumption of molecular oxygen to yield hydrogen peroxide (Scheme 1) (*1*, *2*). NAO is unusual, since it catalyzes substrate oxidation by removing a substrate proton to form a carbanion intermediate (*3*) (Scheme 2), whereas flavoproteins that oxidize carbon−nitrogen and carbon−oxygen bonds typically catalyze cleavage of the substrate carbon−hydrogen bond by removal of a hydride rather than a proton (*4*−*6*). The NAO reaction is initiated by abstraction of the α-proton from the neutral form of the nitroalkane by Asp402, the active site base (*7*), creating a nucleophilic nitroalkane anion (Scheme 2). The anion then attacks the N5 position of FAD to form an adduct; this eliminates nitrite to generate a cationic, electrophilic flavin imine that can be attacked by hydroxide (*8*−*11*). Release of the aldehyde or ketone product forms reduced FAD (*7*). In the more typical oxidative half-reaction, the reduced FAD is oxidized by molecular oxygen to form hydrogen peroxide (*2*). Release of products from the oxidized enzyme limits turnover with primary nitroalkanes,

Scheme 1

the best substrates (*12*). With the slow substrate nitroethane (*13*), formation of the substrate anion is rate-limiting for the reductive half-reaction (*12*).

The proton transfer reaction between nitroethane and Asp402 catalyzed by *F. oxysporum* NAO provides an excellent opportunity for a study of the basis for enzymatic catalysis because the enzymatic process can be modeled by the reaction of nitroethane and acetate in water (*14*). Nitroalkanes represent a prototypical system for the study of carbon acidity, in that they exhibit surprisingly slow deprotonation rates compared with their high acidities, the so-called nitroalkane anomaly (*15*). NAO from *F. oxysporum* catalyzes the ionization of nitroethane 10^9-fold more effectively than acetate. Computations suggest that there is a slight enhancement of quantum mechanical tunneling of the proton in the active site compared to the nonenzymatic reaction (*16*).

NAO is a structural member of the flavoenzyme acyl-CoA dehydrogenase (ACAD) superfamily (*10*, *17*, *18*), even though the sequences of the ACAD family members are only 13−23% identical to that of NAO (*1*, *17*). Both cofactors and the active site bases occupy similar locations in NAO and ACAD, but the substrates access the active site from opposite sides of the two proteins (*11*, *19*). Structural and mutational analyses have identified key active site residues in *F. oxysporum* NAO. The nearest residues to Asp402 are Arg409 and Ser276; together, the three residues make up a catalytic triad. Mutation of Asp402 to alanine decreases the rate constant for abstraction of the

[†]This work was supported in part by NIH Grant GM 058698 to P.F.F. and Robert A. Welch Foundation Grant AQ-1399 to P.J.H.
[‡]The atomic coordinates for PODANSg2158 have been deposited with the Protein Data Bank with the file name 3MKH.
*To whom correspondence should be addressed at the Department of Biochemistry, University of Texas Health Science Center. Phone: (210) 567-8264. Fax: (210) 567-8778. E-mail: Fitzpatrick@biochem.uthscsa.edu.
[1]Abbreviations: NAO, nitroalkane oxidase; Ni-NTA, nickel nitrilotriacetic acid; IPTG, isopropyl thio-2-D-galactopyranoside; DTT, dithiothreitol; EDTA, ethylenediaminetetraacetic acid; Hepes, 4-(2-hydroxyethyl)-1-piperazineethanesulfonic acid; ACAD, acyl-CoA dehydrogenase.

Published on Web 05/18/2010

Scheme 2

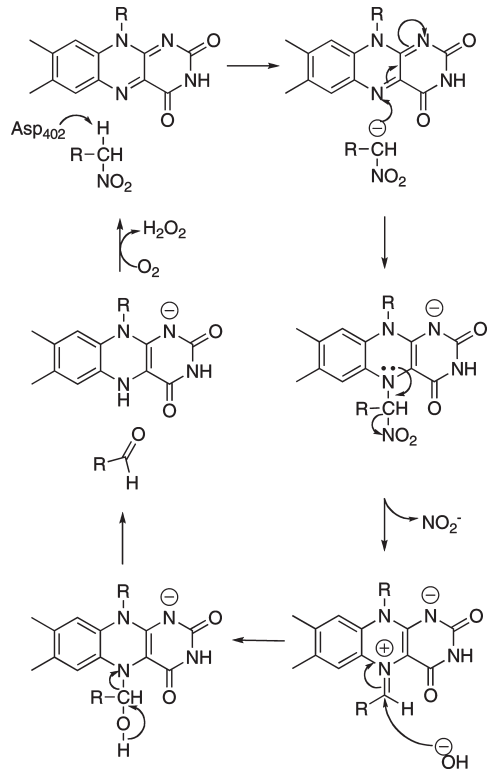

nitroalkane proton by at least 1000-fold (*3*). The distance between Asp402 and Arg409 is appropriate for an electrostatic interaction, suggesting that Arg409 is involved in correctly positioning the active site base for catalysis. Mutation of Arg409 to lysine decreases the rate constant for proton abstraction by 100-fold and alters the position of the active site base (*20*). The side chain hydroxyl of Ser276 forms hydrogen bonds with the carboxylate oxygens of Asp402 (*20*). Mutation of Ser276 to alanine decreases the rate of the proton abstraction by 100-fold without perturbing the active site structure (*11*).

When the sequence of *F. oxysporum* nitroalkane oxidase was first determined, its use as a query in a PSI-BLAST (*21*) search of the available sequence databases identified multiple sequences of acyl-CoA dehydrogenases, establishing the enzyme as related to that family of flavoproteins (*17*). However, all of the sequences identified in such a search contained glutamate as the active site. Since ACADs utilize a glutamate as the active site base (*22*), whereas NAO utilizes aspartate (*7*), all of these enzymes were likely to be true ACADs. The lack of other NAOs rules out the use of sequence analyses to identify residues important for catalysis and to provide insight into the structural basis for the divergent reactions of ACAD and NAO. We report here the identification of several probable NAOs from other fungi and provide kinetic and structural data firmly establishing the hypothetical protein coded by gene PODANSg2158 of *Podospora anserina* as an NAO.

MATERIALS AND METHODS

Materials. FAD, 1-nitroethane, 1-[1,1-$^2H_2$]nitroethane (99% D), 1-nitropropane, 1-nitrobutane, 1-nitropentane, 1-nitrohexane, dimethyl sulfoxide, sodium pyrophosphate, and phenylmethanesulfonyl fluoride were obtained from Sigma-Aldrich (Milwaukee, WI). Dithiothreitol (DTT) was purchased from Inalco Spa (Milan, Italy). Isopropyl thio-2-D-galactopyranoside (IPTG) was purchased from Research Products International Corp. (Prospect, IL). Kanamycin monosulfate was purchased from Fisher Bioreagents (Fair Lawn, NJ). Lysozyme was obtained from Roche Molecular Biochemicals (Indianapolis, IN); ethylenediaminetetraacetic acid (EDTA) was obtained from Acros Organics (Morris Plains, NJ); potassium phosphate and 4-(2-hydroxyethyl)-1-piperazineethanesulfonic acid (Hepes) were obtained from Fisher Scientific (Fair Lawn, NJ). The nickel nitrilotriacetic acid (Ni-NTA) column was obtained from Invitrogen (Carlsbad, CA). Ampicillin was from USB Corp. (Cleveland, OH). The pET21b(+) vector was from Novagen (Madison, WI).

The pJ201:20714 plasmid containing an artificial gene coding for PODANSg2158 (protein XP 001905136.1; GeneID 6189407) from *P. anserina* 980 with codons optimized for expression in *Escherichia coli* was obtained from DNA 2.0 (Menlo Park, CA). Oligonucleotides were synthesized by the Nucleic Acid Core Facility at the University of Texas Health Science Center at San Antonio. Restriction endonucleases and Taq polymerase were purchased from New England Biolabs (Ipswich, MA). T4 ligase and dNTP's were obtained from Promega (Madison, WI). Pfu DNA polymerase was obtained from Stratagene (La Jolla, CA). Plasmids were purified using mini- and midi-kits from Qiagen. *E. coli* strain BL21(DE3) from Novagen was used for protein expression, and strain XL10-Gold (Stratagene) was used during DNA cloning protocols. DNA sequencing was carried out with the Applied Biosystems Big Dye Terminator V3.1 kit and analyzed by the Nucleic Acid Core Facility at the University of Texas Health Science Center at San Antonio. The D399N, R40K, and S273A mutations were generated with the QuikChange site-directed mutagenesis kit (Stratagene).

Expression and Purification of PODANSg2158. The DNA coding for PODANSg2158 was subcloned from pJ201:20714 into pET21b(+) using the *Nco*I and *Eco*RI sites at the 5′ and 3′ ends, respectively, to obtain pPODNE. A single colony of *E. coli* strain BL21(DE3) transformed with pPODNE was used to inoculate 25 mL of LB containing 100 μg/mL ampicillin at 37 °C. The starter culture was grown for 10−12 h; 10 mL was used to inoculate 1 L of LB containing 100 μg/mL ampicillin at 37 °C. When the A_{600} value of the culture reached 0.6, IPTG was added to a final concentration of 0.25 mM, and the temperature of the culture was lowered to 18 °C. After 14−20 h, cells were harvested by centrifugation at 5000*g* and 4 °C for 30 min. The cells were suspended in 10 volumes of 50 mM Hepes, pH 7.0, 1.0 mM EDTA, 0.1 mM FAD, 0.1 mM DTT, 0.5 mM phenylmethanesufonyl fluoride, and 25 μg/mL lysozyme. The suspension was sonicated for 7 min on ice and centrifuged at 12000*g* for 20 min. The extract was loaded onto a Ni-NTA column that had been previously equilibrated with 50 mM Hepes buffer, pH 8.0. The column was eluted with a linear gradient from 0 to 2 M imidazole (200 mL total) in the same buffer. Fractions with the highest purity as judged by UV−visible absorbance and SDS−PAGE were pooled and concentrated using an Amicon Ultra (Millipore) centrifugal filter device. The mutant enzymes were expressed and purified following the same protocol. Purified enzymes were stored with 15% glycerol at −80 °C.

Extinction Coefficient of PODANSg2158. An equal volume of 7 M urea was added to the enzyme in 50 mM Hepes, pH 8.0 (*8*). Any precipitated protein was removed by centrifugation for 10 min at 14000*g*, and the visible absorbance spectrum of the supernatant was recorded. The change in absorbance between the enzyme-bound FAD and the free FAD after denaturation was used to calculate the extinction coefficient of the purified enzyme.

```
PODANSg2158   FGAFDGS--AVLVGAMGVGL     VVLPIFDGGNVGIRRRHLQQ
TSTA 069890   ENSFGMS--AALVGAMSAGI     VCLSLFDGGNVGVRRRQLQQ
PMAA 028790   ENSFGMS--AALVGAMGVGI     ICLSLFDGGNVGVRRRQLQR
FG02379.1     EMAFSFT--AALVGAMACGI     TVLSLFDGGNVGVRRRQYER
SNOG 15929    ERTFGTS--AALVGAMSVGV     ACLPLFDGGNVGVRRRQIEE
CHGG 01268    FGAFDAS--AVLVGAMGVGL     MVLPIFDGGNVGIRRRHLQQ
BC1G 11641    SGSFDCS--AVLVGAMSVSV     IVLPIFDGGNVGIRRRHMQE
SS1G 09730    SRAFDFS--AILVGAMSVSV     IVLPIFDGGNIGIRRRHMQE
NFIA 030710   LHSFEIS--AMLVGAMGVGV     LVLPIFDGGNVGIRRRALQD
AN9162.2      THTFEISETAMLVGAMGVGI     LVLPIFDGGNVGMRRRALQE
NAO           ETAFAMS--AALVGAMAIGT     MCYPLFDGGNIGLRRRQMQR
                   276                       402     409
```

FIGURE 1: Alignment of active site residues of *F. oxysporum* NAO with likely orthologues: PODANSg2158, *P. anserina* DSM 980 hypothetical protein; TSTA 069890, *Talaromyces stipitatus* putative acyl-CoA dehydrogenase; PMAA 028790, *Penicillium marneffei* electron transport oxidoreductase; FG02379.1, *G. zeae* PH-1 hypothetical protein; SNOG 15929, *Phaeosphaeria nodorum* SN15 hypothetical protein; CHGG 01268, *Chaetomium globosum* CBS 148.51 hypothetical protein; BC1G 11641, *Botryotinia fuckeliana* B05.10 hypothetical protein; SS1G 09730, *Sclerotinia sclerotiorum* 1980 hypothetical protein; NFIA 030710, *Neosartorya fischeri* putative acyl-CoA dehydrogenase; AN9162.2, *Aspergillus nidulans* hypothetical protein; NAO, *F. oxysporum* nitroalkane oxidase. Conserved residues are in bold, and the active site catalytic triad Ser276, Asp402, and Arg409 in NAO is in bold and underlined.

Assays. Nitroalkane oxidase activity was routinely measured in 0.5 mM FAD and 50 mM Hepes, pH 8.0, by monitoring the rate of oxygen consumption with a computer-interfaced YSI Model 5300A biological oxygen electrode (YSI Incorporated, Yellow Springs, OH) at 30 °C, as described previously (*23*). When the pH was varied, 50 mM sodium pyrophosphate was used over the pH ranges 5.4−7.0 and 8.0−11.0, and 50 mM potassium phosphate was used between pH 7.0 and pH 8.0. To vary the concentration of oxygen, oxygen and argon were combined in different ratios with a MaxBlend low-flow air/oxygen blender (Maxtec Inc., Salt Lake City, UT), and the assay buffer was equilibrated with the gas mixture. Substrate solutions of nitroalkanes were prepared as stocks in dimethyl sulfoxide to prevent the formation of the anionic substrate. The concentration of active enzyme was determined using an extinction coefficient at 446 nm of 11.9 mM^{-1} cm^{-1}.

Data Analysis. Steady-state kinetic data were analyzed using the programs KaleidaGraph (Synergy Software, Reading, PA) and IgorPro (WaveMetrics, Inc., Lake Oswego, OR). Steady-state kinetic parameters were determined by fitting the data to the Michaelis−Menten equation. The pH dependence of the k_{cat}/K_M value for nitroethane was determined by fitting initial rate data to eq 1, which applies for pH profiles that show a decrease with unit slope at low pH. Here, Y is the k_{cat}/K_{NE} value at a given pH, c is the k_{cat}/K_{NE} value in the pH-independent range, and K_1 is the dissociation constant for the ionization of a group that must be unprotonated for binding or catalysis.

$$\log Y = \log\left(\frac{c}{1+(H/K_1)}\right) \quad (1)$$

Crystallization, Structure Determination, and Refinement. Preliminary crystals of PODANSg2158 were grown in the UTHSCSA X-ray Crystallography Core Laboratory from crystallization screen kits (Qiagen Inc., Valencia, CA) with a Phoenix crystallization robot (Art Robbins Instruments, Sunnyvale, CA). Optimized crystals were grown within 1 week by the vapor diffusion method with the protein solution mixed in a 1:1 ratio with a buffer containing 2.5 M magnesium sulfate, 0.1 M 2-(*N*-morpholino)ethanesulfonic acid buffer, pH 6, and 18% glycerol. The crystals were flash-cooled using liquid nitrogen prior to data collection. Data were collected at the Advanced Photon Source beamline 24-ID-C (Argonne National Laboratory, Argonne, IL) equipped with an ADSC Quantum 315 CCD detector. Data were processed using HKL-2000 (*24*). Phases were generated by the molecular replacement method in PHASER (*25*) using the *F. oxysporum* NAO coordinates in Protein Data Bank entry 2C0U (*10*) as the search model. Coordinates were refined against the data using PHENIX (*26*), including simulated annealing, and alternated with manual rebuilding using COOT (*27*). The coordinates have been deposited in the Protein Data Bank with accession code 3MKH.

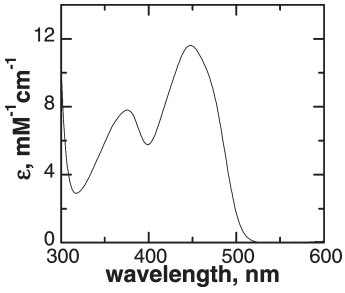

FIGURE 2: UV−visible absorbance spectrum of PODANSg2158. Conditions: 50 mM Hepes at pH 8.0 and 25 °C.

RESULTS

Identification of NAO Orthologues. To identify orthologues of *F. oxysporum* NAO, PSI-BLAST searches of the available sequence databases were carried out. Since the use of aspartate versus glutamate as the active site base readily distinguishes NAO from ACAD, all positive hits containing a glutamate in the position corresponding to Asp402 were discarded. This screen eliminated all plant, bacterial, and vertebrate sequences. However, several fungal proteins fit this initial criterion for NAO orthologues (Figure 1). Their sequence identities to *F. oxysporum* NAO range from 43% to 86%. All contain an arginine corresponding to Arg409 of the *F. oxysporum* enzyme. All but one contain a serine corresponding to Ser276; the lone exception from *Gibberella zeae* contains a threonine in that position. We selected the hypothetical protein from the fungus *P. anserina* 980 coded by gene PODANSg2158 for further study since it has the lowest sequence identity to the *F. oxysporum* enzyme at 43%.

Characterization of PODANSg2158 Expressed in E. coli. The DNA encoding PODANSg2158 was subcloned directly from pJ201:20714 into pET21b(+) using the *Nco*RI and *Eco*RI sites at the 5′ and 3′ ends, respectively, for expression of the His-tagged enzyme. Approximately 40 mg of pure NAO could be obtained from 2 L of culture. The visible absorbance spectrum of the purified enzyme (Figure 2) establishes that the enzyme is a flavoprotein. Based on the small change in absorbance of the

Scheme 3

$$EFAD_{OX} + S \rightleftharpoons EFAD_{OX}S \longrightarrow EFAD_{RED}P_1P_2 \xrightarrow[H_2O_2]{O_2} EFAD_{OX}P_1P_2 \longrightarrow EFAD_{OX} + P_1 + P_2$$

flavin when the protein is denatured, the extinction coefficient of the enzyme at 446 nm is 11.9 mM^{-1} cm^{-1}. The crystal structure of the enzyme shows FAD bound to the active site (see below), establishing this as the form of the cofactor. The purified enzyme is active with nitroethane as the substrate, with a specific activity of 7.5 μmol min^{-1} mg^{-1}. This is comparable to the value of 10.6 μmol min^{-1} mg^{-1} for *F. oxysporum* NAO (*17*). Thus, this protein can be classified as a nitroalkane oxidase.

Steady-State Kinetic Parameters for PODANSg2158. Previous steady-state kinetic analyses of *F. oxysporum* NAO have established the steady-state kinetic mechanism as a modified ping-pong mechanism typical of flavoprotein oxidases (Scheme 3) (*2*, *7*, *28*). Equation 2 gives the appropriate rate equation for such a mechanism. The appropriateness of eq 2 rather than the more complex eq 3 for a sequential mechanism can readily be determined using the fixed ratio method (*29*). In this approach initial rates are measured at different concentrations of the two substrates, keeping the ratio of their concentrations constant. Curvature in a double reciprocal plot of the resulting data suggests a sequential mechanism, since there will be a term containing the square of the concentration of one substrate in the rate equation (eq 4, $a = [O_2]/[NE]$). On the other hand, a linear plot will arise if there is no term in the rate equation containing the concentration of both substrates (eq 5). For PODANSg2158 a double reciprocal plot of initial rate vs nitroethane concentration is linear (Figure 3), establishing eq 2 as appropriate and yielding a k_{cat} value of 15 s^{-1}. For such a mechanism, the k_{cat}/K_M values of the nitroalkane and oxygen are independent of the concentration of the other substrate. The k_{cat}/K_M values for oxygen and nitroethane were determined in separate analyses by varying each at a fixed concentration of the other. These values are given in Table 1. The K_{O_2} value for PODANSg2158 is higher than that for the *F. oxysporum* NAO (*2*) but within the range found for a number of other flavoprotein oxidases (*30*−*34*).

$$\frac{E}{v_0} = \frac{1}{k_{cat}} + \frac{K_{O_2}}{k_{cat}[O_2]} + \frac{K_{NE}}{k_{cat}[NE]} \quad (2)$$

$$\frac{E}{v_0} = \frac{1}{k_{cat}} + \frac{K_{O_2}}{k_{cat}[O_2]} + \frac{K_{NE}}{k_{cat}[NE]} + \frac{K_{NE}K_{O_2}}{k_{cat}[NE][O_2]} \quad (3)$$

$$\frac{E}{v_0} = \frac{1}{k_{cat}} + \frac{K_{O_2}}{k_{cat}a[NE]} + \frac{K_{NE}}{k_{cat}[NE]} + \frac{K_{NE}K_{O_2}}{k_{cat}a[NE]^2} \quad (4)$$

$$\frac{E}{v_0} = \frac{1}{k_{cat}} + \frac{K_{O_2}}{k_{cat}a[NE]} + \frac{K_{NE}}{k_{cat}[NE]} \quad (5)$$

F. oxysporum NAO prefers linear nitroalkanes as substrates, with primary nitroalkanes of four or more carbons having the highest activity. To probe the substrate specificity of the *P. anserina* enzyme, the k_{cat}/K_M values for a number of unbranched primary nitroalkanes were determined. As shown in Figure 4 the latter enzyme also prefers longer nitroalkanes, with 1-nitrohexane having the highest activity. However, this enzyme does not show the monotonic increase in the k_{cat}/K_M value with substrate chain length that *F. oxysporum* NAO does.[2]

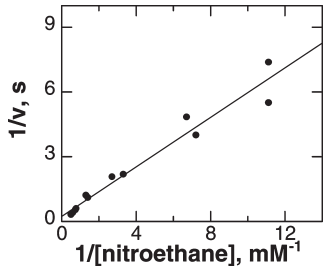

FIGURE 3: Double reciprocal plot of the initial velocity vs the concentration of nitroethane at a fixed ratio of nitroethane to oxygen of 2 at pH 8.0 and 30 °C.

pH Dependence of k_{cat}/K_{NE}. The effect of pH on the k_{cat}/K_M value with nitroethane as substrate for PODANSg2158 was determined in order to obtain information about amino acid residues important for binding and catalysis in that enzyme. Figure 5 shows that the k_{cat}/K_{NE} value is constant at high pH and decreases at low pH, resulting in a pK_a of 5.9 ± 0.1. In comparison the pK_a for *F. oxysporum* NAO is 6.9 ± 0.1 (*12*).

Mutagenesis of Active Site Residues. To probe the role of the catalytic triad in PODANSg2158 (Asp399, Arg406, and Ser273), these residues were replaced with asparagine, lysine, and alanine, respectively. The steady-state kinetic parameters of the mutant enzymes with nitroethane are listed in Table 1. The largest decrease was observed for the mutation of Asp399, as there is a 400-fold decrease in k_{cat} and ~200-fold decrease in the k_{cat}/K_M for nitroethane. The effect on the k_{cat} value is a more valid measure of the effect on the activity, in that the very low activity of this mutant enzyme makes accurate measurement of a k_{cat}/K_{NE} value difficult. Mutagenesis of Arg406 to lysine results in only a 1.7-fold decrease in k_{cat} and a 24-fold decrease in k_{cat}/K_{NE}. Mutation of the Ser273 to alanine results in only a decrease of ~3-fold for both the k_{cat} and k_{cat}/K_{NE} values.

Crystal Structure of PODANSg2158. In order to provide a more complete identification of the *P. anserina* enzyme as an NAO, we determined the three-dimensional structure of the wild-type enzyme by X-ray crystallography. The data collection and refinement are reported in Table 2. The crystallization conditions were different from those used for *F. oxysporum* NAO, yielding crystals that diffracted to 2.0 Å resolution. The protein crystallized in space group $P4_3$, with four subunits in the asymmetric unit, consistent with the tetrameric structure of *F. oxysporum* NAO (*10*). The structure was determined by molecular replacement using the structure of that enzyme as the search model (*10*). FAD could be clearly identified in each of the subunits. Figure 6 shows an overlay of the electron density map with the FAD and active site residues. This figure also shows the chain of ordered water molecules that extends from the FAD 2′-hydroxyl to the protein surface through a different tunnel than the substrate binding site. A similar water chain is seen the structure of *F. oxysporum* enzyme, where it has been proposed to be involved in accepting the proton from the water molecule that forms the hydroxide required in the mechanism in Scheme 2 (*11*). Figure 7 depicts an overlay of the carbon backbones for one subunit from

[2]Longer chain nitroalkanes are poorly soluble in aqueous solutions and therefore were not characterized as substrates.

Table 1: Steady-State Kinetic Parameters for Wild-Type and Mutant PODANSg2158 with Nitroethane as Substrate[a]

kinetic parameter	wild type	D399N	R406K	S273A
k_{cat} (s^{-1})	15 ± 1 (9.3 ± 0.7)[b]	0.037 ± 0.009[b]	9.0 ± 0.5[b]	5.0 ± 0.3[b]
K_{NE} (mM)	13 ± 4	10 ± 8[b]	25 ± 4[b]	24 ± 4[b]
k_{cat}/K_{NE} (mM^{-1} s^{-1})[b]	0.74 ± 0.20	0.004 ± 0.002	0.37 ± 0.04	0.21 ± 0.02
K_{O_2} (mM)[c]	0.39 ± 0.08			
k_{cat}/K_{O_2} (mM^{-1} s^{-1})[c]	38 ± 5			

[a]Conditions: 50 mM Hepes, pH 8.0, 30 °C. [b]Determined by varying the concentration of nitroethane at 247 μM oxygen. [c]Determined by varying the concentration of oxygen at 50 mM nitroethane.

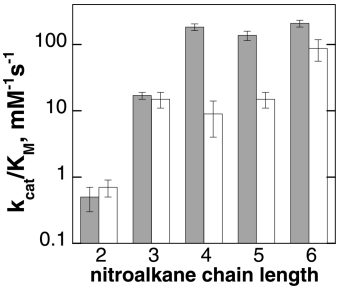

FIGURE 4: Nitroalkane substrate specificities for *F. oxysporum* NAO and PODANSg2158. Conditions for PODANSg2158: 50 mM Hepes, pH 8.0 at 30 °C (empty bars). Data for *F. oxysporum* NAO from Gadda et al. (*12*) (filled bars).

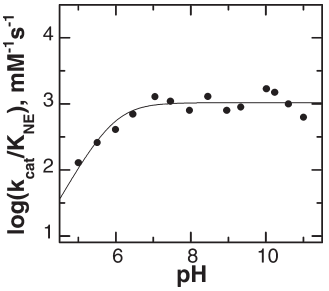

FIGURE 5: k_{cat}/K_M−pH profile for PODANSg2158 with nitroethane as substrate. The line is from a fit of the data to eq 3.

Table 2: Data Collection and Refinement Statistics

data collection	
space group	$P4_3$
cell dimensions	
a, *b*, *c* (Å)	137.5, 137.5, 131.3
α, β, γ (deg)	90, 90, 90
wavelength	0.97949
resolution (Å)	50−2.0
R_{sym}[a]	0.089 (0.589)
I/σI	17.7 (3.3)
completeness (%)	99.7 (100)
redundancy	6.2 (6.1)
refinement	
resolution (Å)	44.9−2.0
no. of reflections	152266
R_{work}/R_{free}	0.176/0.209
no. of atoms	
protein	12660
ligand	224
solvent	1431
rms deviations[b]	
bond lengths (Å)	0.011
bond angles (deg)	1.217

[a]Values in parentheses are for the highest resolution shell. [b]Rms deviations are from idealized values for protein.

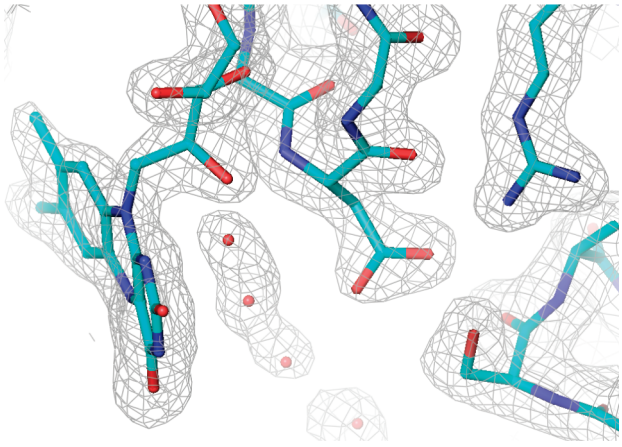

FIGURE 6: The PODANSg2158 active site superimposed on σA-weighted electron density with coefficients $2mF_o - DF_c$ contoured at 1.2σ. The FAD isoalloxazine ring, the catalytic triad consisting of residues S273, D399, and R406, and a chain of hydrogen-bonded water molecules running from the active site to the bulk solvent are shown.

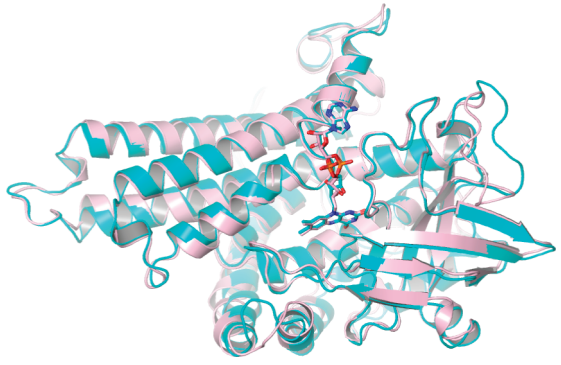

FIGURE 7: Superposition of subunit A of the *F. oxysporum* NAO structure [PDB code 2C12 (*10*), pink] and subunit A of the PODANSg2158 structure (cyan). The respective flavins are shown in stick representation with the same color scheme.

each enzyme. The two proteins clearly have the same overall fold; this is confirmed by the rmsd of 0.925 over 376 residues. An overlay of the catalytic triad from *P. anserina* and *F. oxysporum* NAOs, as well as the bound FAD, is shown in Figure 8. The positions of the FAD and the active site residues are conserved in the two enzymes.

DISCUSSION

The results described here identify PODANSg2158 as an NAO. The enzyme is a flavoprotein, and the steady-state kinetic parameters in Table 1 establish the enzyme has nitroalkane oxidase activity. The identities between the *P. anserina* and *F. oxysporum* NAO are spread through the sequence; more

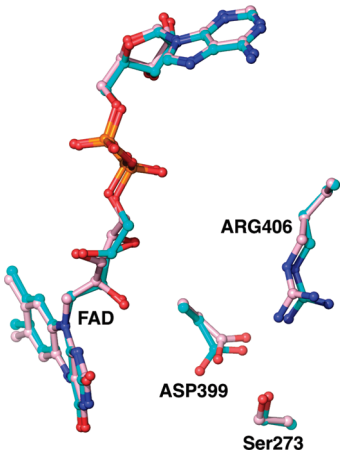

FIGURE 8: Overlay of the active sites from PODANSg2158 (carbon atoms colored in pink) and *F. oxysporum* NAO (carbon atoms colored in cyan). The active site of PODANSg2158 was overlaid with that of *F. oxysporum* enzyme (PDB code 2C12) (*10*) by superimposing the four carbons on the central ring in the FADs.

importantly, the active site aspartate (Asp399/402), arginine (Arg406/409), and serine (Ser273/276) are conserved. The very similar three-dimensional structures confirm the assignment. These results suggest that the remaining proteins with sequences in Figure 1 can also be described as nitroalkane oxidases. NAO was previously proposed to be a member of the ACAD superfamily distinct from acyl-CoA dehydrogenases and acyl-CoA oxidases (*1*, *17*), and SCOP (*35*) classifies NAO as a member of the medium-chain acyl-CoA dehydrogenase-like family, despite the low (~25%) sequence identity to other members of the family. The distinct activities of NAO and acyl-CoA dehydrogenases and the very different active site residues suggest that NAO and related enzymes are better classified as a separate family within the superfamily. *F. oxysporum* NAO has been a model system for understanding enzyme-catalyzed carbanion formation (*16*, *36*). The availability of NAOs from additional sources expands the utility of the enzyme as a model system.

While PODANSg2158 is clearly an NAO, this enzyme differs from *F. oxysporum* NAO in a number of properties. The latter enzyme prefers linear primary nitroalkanes as substrates (*13*). There is an increase in the k_{cat}/K_M with each additional methylene group of the substrate up to 1-nitrobutane due to an increase in the forward commitment with increasing chain length and a decrease of 16-fold in the K_d with each additional methylene group (*12*). PODANSg2158 is similarly more active on longer nitroalkanes, but the increase in the k_{cat}/K_M values suggests a preference for longer chains than is the case for the *F. oxysporum* enzyme. Figure 9 (top) shows the active site of NAO with 1-nitrooctane bound. The substrate binds near the flavin at the end of a tunnel that extends to the protein surface (*11*). The nitroalkane binding pocket fits 1-nitrooctane well, with a constriction in the tunnel just distal of the terminal carbon of the substrate. PODANSg2158 has a similar tunnel, as shown in Figure 9 (bottom). Comparison of the nitroalkane binding cavities and the tunnels in the two enzymes shows that the tunnel in PODANSg2158 is much more open. This structural difference provides a reasonable explanation for the differences in substrate specificities of the two enzymes.

A key distinction between an NAO and the acyl-CoA dehydrogenases and oxidases that are also in the ACAD superfamily is the use of an aspartate as the active site base in

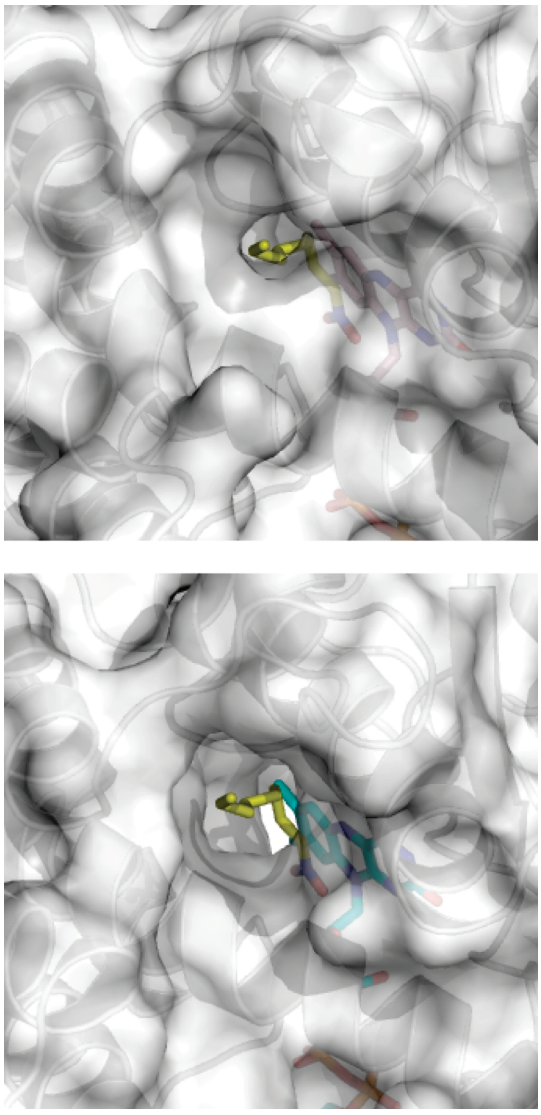

FIGURE 9: Active site entrances in *F. oxysporum* nitroalkane oxidase [PDB code 2C12 (*10*), top] and *P. anserina* PODANSg2158 (bottom). The placement of the 1-nitrooctane (yellow in both panels) is based on the superposition of the backbone atoms of these structures with the backbone atoms of PDB code 2D9E (*11*).

NAO and a glutamate in ACADs. Asp402 is the active site base in *F. oxysporum* NAO, with a pK_a of 6.9 in the free enzyme (*3*). Mutagenesis of this residue to alanine or asparagine decreases the rate constant for proton abstraction by 3 orders of magnitude. The structural and kinetic data presented here establish that Asp399 is the active site base in PODANSg2158. The decrease in the k_{cat} of the D399N enzyme of 400-fold provides a lower limit for the effect; with the *F. oxysporum* enzyme, product release is rate-limiting for turnover, so that decreases in the rate constant for CH bond cleavage are not fully reflected in the k_{cat} value (*7*). The pK_a of 5.9 in the k_{cat}/K_{NE} profile for PODANSg2158 can reasonably be assigned to Asp399. It cannot be established from the present data whether the differences in the pK_a values of the bases in the two enzymes truly differ by one pK unit, since the pK_a value for PODANSg2158 could be perturbed by a significant commitment to catalysis with nitroethane as substrate. In the case of the *F. oxysporum* enzyme, the pK_a of 6.9 seen with nitroethane shifts to lower values with longer chain nitroalkanes due to increasing commitment with increased chain length (*12*).

While the active site triad of an aspartate interacting with an arginine and a serine is maintained in PODANSg2158, the effects of mutating the arginine and serine are less in PODANSg2158 than in *F. oxysporum* NAO. In the latter enzyme, the R409K and S276A mutations decrease the k_{cat}/K_{NE} value by 64-fold and 21-fold, respectively (*11*, *20*), compared to decreases of 24-fold and 3-fold observed here. A significant forward commitment to catalysis could decrease the effect of mutating an active site residue, in addition to perturbing the pK_a value seen in the k_{cat}/K_{NE}−pH profile, since CH bond cleavage would no longer be fully rate-limiting for nitroethane oxidation.

In summary, the data presented here establish that PODANSg2158, designated as a hypothetical protein in the sequence database, is better classified as a nitroalkane oxidase. They also suggest that the presence of the active site aspartate, arginine, and serine discriminates between NAOs and true ACADs.

ACKNOWLEDGMENT

This work is based upon research conducted at the Northeastern Collaborative Access Team beamlines of the Advanced Photon Source, supported by award RR-15301 from the National Center for Research Resources at the National Institutes of Health. Use of the Advanced Photon Source is supported by the U.S. Department of Energy, Office of Basic Energy Sciences, under Contract No. W-31-109-ENG-38. We thank Dr. Jonathan P. Schuermann at the Advanced Photon Source for collecting the X-ray diffraction data. Support for the X-ray Crystallography Core Laboratory by the UTHSCSA Executive Research Committee and the San Antonio Cancer Institute is also gratefully acknowledged.

REFERENCES

1. Fitzpatrick, P. F., Orville, A. M., Nagpal, A., and Valley, M. P. (2005) Nitroalkane oxidase, a carbanion-forming flavoprotein homologous to acyl-CoA dehydrogenase. *Arch. Biochem. Biophys. 433*, 157–165.
2. Heasley, C. J., and Fitzpatrick, P. F. (1996) Kinetic mechanism and substrate specificity of nitroalkane oxidase. *Biochem. Biophys. Res. Commun. 225*, 6–10.
3. Valley, M. P., and Fitzpatrick, P. F. (2003) Inactivation of nitroalkane oxidase upon mutation of the active site base and rescue with a deprotonated substrate. *J. Am. Chem. Soc. 23*, 8738–8739.
4. Fitzpatrick, P. F. (2004) Carbanion versus hydride transfer mechanisms in flavoprotein-catalyzed dehydrogenations. *Bioorg. Chem. 32*, 125–139.
5. Fitzpatrick, P. F. (2010) Oxidation of amines by flavoproteins. *Arch. Biochem. Biophys. 493*, 13–25.
6. Gadda, G. (2008) Hydride transfer made easy in the reaction of alcohol oxidation catalyzed by flavin-dependent oxidases. *Biochemistry 47*, 13745–13753.
7. Valley, M. P., and Fitzpatrick, P. F. (2003) Reductive half-reaction of nitroalkane oxidase: effect of mutation of the active site aspartate to glutamate. *Biochemistry 42*, 5850–8566.
8. Gadda, G., Edmondson, R. D., Russel, D. H., and Fitzpatrick, P. F. (1997) Identification of the naturally occurring flavin of nitroalkane oxidase from *Fusarium oxysporum* as a 5-nitrobutyl-FAD and conversion of the enzyme to the active FAD-containing form. *J. Biol. Chem. 272*, 5563–5570.
9. Valley, M. P., Tichy, S. E., and Fitzpatrick, P. F. (2005) Establishing the kinetic competency of the cationic imine intermediate in nitroalkane oxidase. *J. Am. Chem. Soc. 127*, 2062–2066.
10. Nagpal, A., Valley, M. P., Fitzpatrick, P. F., and Orville, A. M. (2006) Crystal structures of nitroalkane oxidase: insights into the reaction mechanism from a covalent complex of the flavoenzyme trapped during turnover. *Biochemistry 45*, 1138–1150.
11. Héroux, A., Bozinovski, D. M., Valley, M. P., Fitzpatrick, P. F., and Orville, A. M. (2009) Crystal structures of intermediates in the nitroalkane oxidase reaction. *Biochemistry 48*, 3407–3416.
12. Gadda, G., Choe, D. Y., and Fitzpatrick, P. F. (2000) Use of pH and kinetic isotope effects to dissect the effects of substrate size on binding and catalysis by nitroalkane oxidase. *Arch. Biochem. Biophys. 382*, 138–144.
13. Gadda, G., and Fitzpatrick, P. F. (1999) Substrate specificity of a nitroalkane oxidizing enzyme. *Arch. Biochem. Biophys. 363*, 309–313.
14. Valley, M. P., and Fitzpatrick, P. F. (2004) Comparison of enzymatic and non-enzymatic nitroethane anion formation: thermodynamics and contribution of tunneling. *J. Am. Chem. Soc. 126*, 6244–6245.
15. Bernasconi, C. F. (1992) The principle of non-perfect synchronization. *Adv. Phys. Org. Chem. 27*, 119–238.
16. Major, D. T., Heroux, A., Orville, A. M., Valley, M. P., Fitzpatrick, P. F., and Gao, J. (2009) Differential quantum mechanical tunneling in the uncatalyzed and in the nitroalkane oxidase catalyzed proton abstraction of nitroethane. *Proc. Natl. Acad. Sci. U.S.A. 106*, 20734–20739.
17. Daubner, S. C., Gadda, G., Valley, M. P., and Fitzpatrick, P. F. (2002) Cloning of nitroalkane oxidase from *Fusarium oxysporum* identifies a new member of the acyl-CoA dehydrogenase superfamily. *Proc. Natl. Acad. Sci. U.S.A. 99*, 2702–2707.
18. Kim, J. J., and Miura, R. (2004) Acyl-CoA dehydrogenases and acyl-CoA oxidases. Structural basis for mechanistic similarities and differences. *Eur. J. Biochem. 271*, 483–493.
19. Thorpe, C., and Kim, J. P. (1995) Structure and mechanism of action of the acyl-CoA dehydrogenases. *FASEB J. 9*, 718–725.
20. Fitzpatrick, P. F., Valley, M. P., Bozinovski, D. M., Shaw, P. G., Héroux, A., and Orville, A. M. (2007) Mechanistic and structural analyses of the roles of Arg409 and Asp402 in the reaction of the flavoprotein nitroalkane oxidase. *Biochemistry 46*, 13800–13808.
21. Altschul, S. F., Madden, T. L., Schäffer, A. A., Zhang, J., Zhang, Z., Miller, W., and Lipman, D. J. (1997) Gapped BLAST and PSI-BLAST: a new generation of protein database search programs. *Nucleic Acids Res. 25*, 3389–3402.
22. Ghisla, S., and Thorpe, C. (2004) Acyl-CoA dehydrogenases. A mechanistic overview. *Eur. J. Biochem. 271*, 494–508.
23. Gadda, G., and Fitzpatrick, P. F. (1998) Biochemical and physical characterization of the active FAD-containing form of nitroalkane oxidase from *Fusarium oxysporum*. *Biochemistry 37*, 6154–6164.
24. Otwinowski, Z., and Minor, W. (1997) Processing of X-ray diffraction data collected in oscillation mode. *Methods Enzymol. 276*, 307–326.
25. McCoy, A. J., Grosse-Kunstleve, R. W., Adams, P. D., Winn, M. D., Storoni, L. C., and Read, R. J. (2007) Phaser crystallographic software. *J. Appl. Crystallogr. 40*, 658–674.
26. Adams, P. D., Afonine, P. V., Bunkóczi, G., Chen, V. B., Davis, I. W., Echols, N., Headd, J. J., Hung, L.-W., Kapral, G. J., Grosse-Kunstleve, R. W., McCoy, A. J., Moriarty, N. W., Oeffner, R., Read, R. J., Richardson, D. C., Richardson, J. S., Terwilliger, T. C., and Zwart, P. H. (2010) PHENIX: a comprehensive Python-based system for macromolecular structure solution. *Acta Crystallogr. D 66*, 213–221.
27. Emsley, P., and Cowtan, K. (2004) Coot: model-building tools for molecular graphics. *Acta Crystallogr., Sect D: Biol. Crystallogr. 60*, 2126–2132.
28. Gadda, G., and Fitzpatrick, P. F. (2000) Mechanism of nitroalkane oxidase: 2. pH and kinetic isotope effects. *Biochemistry 39*, 1406–1410.
29. Rudolph, F. B., and Fromm, H. J. (1979) Plotting methods for analyzing enzyme rate data. *Methods Enzymol. 63*, 138–159.
30. Dixon, M., and Kleppe, K. (1965) D-Amino acid oxidase. II. Specificity, competitive inhibition and reaction sequence. *Biochim. Biophys. Acta 96*, 368–382.
31. Newton-Vinson, P., Hubalek, F., and Edmondson, D. E. (2000) High-level expression of human liver monoamine oxidase B in *Pichia pastoris*. *Protein Expression Purif. 20*, 334–345.
32. Zhao, G., Song, H., Chen, Z., Mathews, S., and Jorns, M. S. (2002) Monomeric sarcosine oxidase: role of histidine 269 in catalysis. *Biochemistry 41*, 9751–9764.
33. Gaweska, H., Henderson Pozzi, M., Schmidt, D. M. Z., McCafferty, D. G., and Fitzpatrick, P. F. (2009) Use of pH and kinetic isotope effects to establish chemistry as rate-limiting in oxidation of a peptide substrate by LSD1. *Biochemistry 48*, 5440–5445.
34. Henderson Pozzi, M., and Fitzpatrick, P. F. (2010) A lysine conserved in the monoamine oxidase family is involved in oxidation of the reduced flavin in mouse polyamine oxidase. Arch. Biochem. Biophys. (in press).
35. Murzin, A. G., Brenner, S. E., Hubbard, T., and Chothia, C. (1995) SCOP: a structural classification of proteins database for the investigation of sequences and structures. *J. Mol. Biol. 247*, 536–540.
36. Major, D. T., York, D. M., and Gao, J. (2005) Solvent polarization and kinetic isotope effects in nitroethane deprotonation and implications to the nitroalkane oxidase reaction. *J. Am. Chem. Soc. 127*, 16374–16375.